Structural Eng. / Earthquake Eng. Vol. 6. No. 1, 13s- 21s. April 1989
Japan Society of Civil Engineers (Proc. of JSCE No. 404/I-11)

EVALUATION OF SCATTER IN FATIGUE LIFE OF WELDED DETAILS USING FRACTURE MECHANICS

By Kentaro YAMADA and Shogo NAGATSU***

Scatter in fatigue life of various welded details is an important factor to be considered in fatigue design codes. The fatigue crack propagation life of two welded details, such as non-load-carrying fillet welded specimens and welded beams, is computed using fracture mechanics. Monte Carlo simulation technique is used to define the initial conditions, such as crack sizes, weld toe geometries, crack shapes, and blowhole sizes. The probability distributions of those parameters are obtained from the actual measurements. The analytical results are generally in good agreement with the experimental results. They are also compared with the allowable stresses given in the fatigue design codes.

Keywords : fatigue, fracture mechanics, welded joints, Monte Carlo simulation

1. INTRODUCTION

To carry out the fatigue assessment of structures, reasonably accurate estimation of service stresses and the fatigue strength of standard welded joints are essential. Normally, the design S-N diagram is obtained from fatigue tests. Constant amplitude fatigue tests are conducted on specimens that represent structural details of interest and the fatigue data with scatters are analyzed statistically. We have obtained numerous fatigue test data in the past[1]. However, the constant amplitude fatigue test data for a long fatigue life range, such as the data more than ten million cycles, are not always available at present because of the enormous amount of time and money needed. Since there exist some welded joints that are subjected to more than five million cycles of loading in their life span, the fatigue tests and analyses on the long fatigue life range are currently under way. It includes the study on the variable amplitude fatigue.

This study aims at developing the analytical technique to compute crack propagation life, N_p, to evaluate the scatter of fatigue life. The probability distribution of the influential parameters that affect the scatter of fatigue life, such as initial crack sizes and weld toe profiles, were obtained based on the actual measurements. The scatter of these parameters were then given as the initial conditions of the analysis using the Monte Carlo simulation technique. The analysis of crack propagation life was carried out using these initial conditions and the scatter of fatigue crack propagation life was evaluated. The threshold value of stress intensity factor range, ΔK_{th}, was introduced to evaluate the fatigue behavior on the long fatigue life region, where the number of loading was more than five million cycles.

* Member of JSCE, Ph. D., Associate Professor, Department of Civil Engineering, Nagoya University (Furocho, Chikusaku, Nagoya 464-01)
* Member of JSCE, M. Eng., Kawasaki Steel Co., Formerly, Graduate Student, Nagoya University.

2. FATIGUE LIFE ANALYSIS AND MONTE CARLO SIMULATION TECHNIQUE

(1) Evaluation of crack propagation life using fracture mechanics

Normally fatigue life, N_f, can be defined as the sum of the crack initiation life, N_c, and the crack propagation life, N_p. In the case of welded joints, fatigue crack initiates at the early stage of fatigue life. For example, fatigue cracks propagated from blow holes in longitudinal fillet welds almost from the first cycle of loading[12),13)]. Fatigue cracks of less than 0.2 mm deep were also detected at the fillet weld toes at less than 20 percent of N_f[2)]. Therefore, the N_c may be negligible compared with the N_f. By neglecting the N_c, one will get a fatigue life close to the lower bound of N_f. The fatigue design specifications also adopt the mean-2s fatigue life (s : standard deviation) for the design S-N diagram[3),4)]. Thus the assumption of $N_f \fallingdotseq N_p$ is justified for welded joints with rather high stress concentration. Since the N_p can be computed by using a fracture mechanics technique, the N_f used for design S-N diagrams can also be derived from such computation.

The fracture mechanics technique is given by the following empirical equations relating the stress intensity factor range, ΔK (MPa$\sqrt{\text{m}}$), which characterizes the stress states at the crack tip, the threshold value of stress intensity factor range, ΔK_{th} (the cracks do not propagate when ΔK is below ΔK_{th}), and the crack growth rate, da/dn (mm/cycle) :

$$da/dn = C(\Delta K^m - \Delta K_{th}^m) \quad \cdots\cdots (1)$$

In this study, the mean values of constants C, m and ΔK_{th} in Eq. (1) for the weld metal of SM 50 steel were used[5)]. They were $C=9.69\times10^{-9}$, $m=2.9$, and $\Delta K_{th}=2.5$ MPa$\sqrt{\text{m}}$. They were obtained from center notched specimens tested at stress ratio of $R=0$. The number of cycles for a fatigue crack propagation can be computed by integrating from an initial crack length, a_0, to a final crack length, a_f.

The stress intensity factor range ΔK for the crack in welded joints can be expressed as follows[6)].

$$\Delta K = \sigma_r\sqrt{\pi a}\, F_s F_e F_t F_g \quad \cdots\cdots (2)$$

where σ_r is the stress range (the difference between the maximum stress and the minimum stress) and a is the crack length. F_s, F_e, F_t and F_g are the correction factors for a free surface, for an elliptical crack shape, for a finite plate thickness, and for a stress gradient, respectively[6)].

(2) Monte Carlo simulation technique

In order to evaluate the effects of the scatter in influential parameters, such as the initial crack sizes and weld toe profiles, on the fatigue life, the actual measurements of these parameters were investigated. Based on the measured data, the probability distributions were given to those parameters. They were then assigned by using the Monte Carlo simulation technique and the analysis of fatigue crack propagation were carried out. The simulation results were compared with the corresponding lower bound values given in the fatigue design specifications with 95 % confidence interval.

The convergent property and the number of simulation were determined in the following way. The simulation analysis was first carried out on non-load-carrying fillet welded joints twice at the same stress range level. The number of simulations was 20 000. An average value with 95 % confidence interval of N_p in two simulations was defined as the standard value $N^*_{p2.5}$. The error, e, caused by the smaller number of simulations was defined by the following equation :

$$e = (\log N_{p2.5} - \log N^*_{p2.5})/\log N^*_{p2.5} \times 100 \quad \cdots\cdots (3)$$

where $N_{p2.5}$ is the lower bound value of the N_p with 95 % confidence interval for any simulations. The results are shown in Fig. 1. When the stress range is high, small number of simulation gives satisfactory results. Even for small stress range levels, the error is below 0.5 %, if the number of simulation is over 1 000. Thus the number of simulation was determined as 1 000 for all cases.

3. EVALUATION ON NON-LOAD-CARRYING FILLET WELDED JOINTS

(1) Analytical model of non-load-carrying fillet welded joints in tension

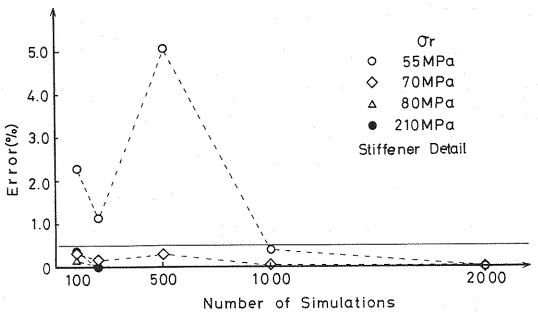

Fig. 1 Number of simulation versus error relation for the lower confidence values of N_p.

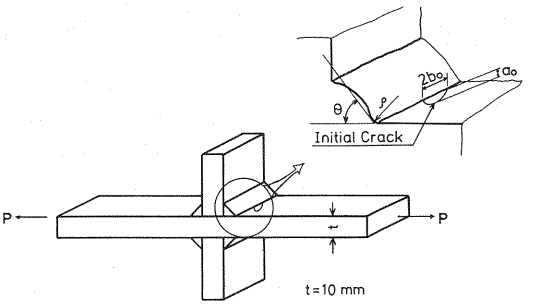

Fig. 2 Typical test specimen for non-load-carrying fillet weld. Fatigue cracks normally initiate at the weld toe.

The non-load-carrying fillet welded joint subjected to tensile stress, shown in Fig. 2, is normally used as a model in fatigue tests[2]. The analytical model consists of 10 mm thick main plate with fillet welded ribs of 10 mm thick. The leg length of fillet welds is 6 mm. The fatigue crack initiates at the fillet weld toe and propagate in a semi-elliptical shape towards the thickness direction. The initial crack length, a_0, the flank angle, θ, the toe radius, ρ, and the shape of crack (aspect ratio), a/b, are the influential factors that affect the fatigue strength[2),7),8)]. The correction factors of stress intensity factor for the semi-elliptical crack are defined as follows:

$$F_s=1.12-0.12\,a/b \quad (4)$$

$$F_e=1/E_K,\ E_K=\int_0^{\pi/2}(1-k^2\sin^2\phi)\,d\phi,\ k^2=1-(a/b)^2 \quad (5)$$

$$F_t=\sqrt{2t/\pi a\tan(\pi a/2t)} \quad (6)$$

where a and b are a crack depth and a half of crack width, respectively. As for the geometry correction factor, F_g, the results obtained by Yamada, et al. were used[2]. The results were obtained from stress analysis using the finite element method, on twelve combinations of toe radius, ρ and flank angle, θ, in non-load-carrying fillet welded joints. The F_g values for any weld toe profile are given in the analysis by interpolating the known F_g values for the twelve cases of the combination of ρ and θ.

(2) Evaluation to influential parameters

Initial crack length a_0: —It is difficult to define the initial crack at the toe of non-load-carrying fillet weld unless defects such as undercuts are assumed. Engesvik assumed that the initial cracks can be defined by the following log-normal distribution[9),10)], where $x=a_0$. He obtained the values $A=0.350$ and $B=2.143$ in Eq. (7) according to the collected data of the initial crack length for welds containing undercut and slag inclusion, etc.

$$f(x)=\frac{1}{\sqrt{2\pi}\cdot Ax}\exp\left\{-\frac{1}{2}\left(\frac{\ln x+B}{A}\right)^2\right\} \quad (7)$$

This distribution is shown in Fig. 3(a). In the analysis, the upper bound was assumed to be 0.4 mm, considering that repairing would be made when the initial defect was too large. The lower bound of 0.075 mm was also introduced. It is due to the fact that some irregularities at the as-welded fillet weld toes exist and it seems reasonable to assume that an initial crack size larger than 0.075 mm always exists along the fillet weld toe. Fatigue crack propagation analysis of non-load-carrying fillet welded joints in the past normally used the value $a_0=0.2$ mm[7),8)]. The Standard Specifications for Highway Bridges specifies that the undercut at the fillet weld toe should be less than 0.3 mm[11)].

Flank angle θ: —The flank angle of fillet weld toe can be measured by using Silicon compound used by the dentist. Although some measurements can be found in the literatures, little measurement has been carried out to show the weld toe shape at crack initiation points. Tagaki, et al. measured the weld toe

shapes of 29 fillet welded specimens, both at the crack initiation points and the other 20 points for each specimens[8]. The histogram of the data and the probability distribution are shown in Fig. 3(b). This can be expressed by the log-normal distribution, as shown in Eq. (7), and the coefficients $A=0.29$ and $B=-3.62$ were obtained. The flank angle was assumed to vary from 20 degree to 65 degree.

Toe radius ρ : —Toe radius can be measured in the same manner as flank angle by using Silicon compound. The histogram of ρ and its probability distribution at crack initiation points, measured by Tagaki, et al.[4], are shown in Fig. 3(c). It was observed qualitatively that the smaller toe radius had large influence on crack initiation. Since the number of occurrence was maximum at $\rho=0.3$ mm, it was assumed that the mean value of the log-normal distribution was 0.33 mm ($A=0.86$, $B=1.10$ in Eq. (7)). The upper bound value of ρ was assumed as 3 mm, because ρ did not exceed such a value in as-welded condition.

Initial crack shape (aspect ratio), a/b : —The crack shape, a/b, normally varies as the crack propagates. As shown in Fig. 4, Tagaki, et al.[8] and Albrecht, et al.[2] studied the relationship between the crack length, a, and the half of the crack width, b, for non-load-carrying fillet welded joints. Since the initial crack length was assumed to vary from 0.075 mm to 0.4 mm, crack shapes in this range were regarded as initial crack shapes. Their histogram and probability distribution are shown in Fig. 3(d). The log-normal distribution of Eq. (7) was assumed to express the initial crack shape with $A=0.40$ and $B=1.01$. The logarithmic mean value of this distribution was 0.36, and the maximum and the minimum values of 0.14 and 0.73 were also used. In addition, Yamada, et al. showed that the shape of cracks initiated at the toe of non-load-carrying fillet welded joints converged to $a/b=1/3$[2),7)]. For simplicity in the analysis, it was assumed that the crack shape remained unchanged until the crack length reached 1 mm, and then the crack gradually changed its shape into $a/b=1/3$ at $a=9$ mm, as shown in Fig. 4.

(3) Sensitivity analysis

Sensitivity analysis was carried out on each parameter shown above by giving the probability distribution. The other three parameters remained constant at their mean values. The histograms of N_p at the sensitivity analysis for the stress range of 80 MPa and 210 MPa are shown in Fig. 5. When the stress range $\sigma_r=210$ MPa, the mean value of the N_p is about 160 000 cycles, and the coefficient of variance decreases in the order of crack shape, toe radius, flank angle, and initial crack length. In the case of $\sigma_r=80$ MPa the results are different due to the influence of ΔK_{th}.

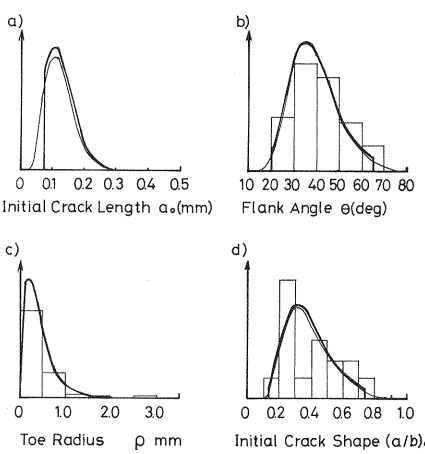

Fig. 3 Distributions for a) initial crack sizes, b) flank angles, c) toe radius, d) initial crack shape. The thick solid lines indicate the distribution used in the analysis considering the upper and the lower limits.

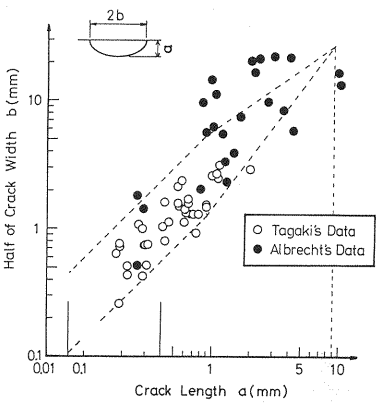

Fig. 4 Measured crack shapes during crack propagation stage. The dotted lines show the upper and the lower bound of the assumed crack shapes during propagation.

The mean value of the N_p is about 3 million cycles; the coefficient of variance is larger than in the case of σ_r=210 MPa and decreases in the order of toe radius, flank angle, crack shape and initial crack length. When the distribution is given to the toe radius and flank angle, the runout data appears and the coefficient of variance increases.

(4) Simulation results

Considering the scatter of each parameter stated above, the simulation analysis was carried out on nine levels of stress ranges ranging from 45 MPa to 210 MPa. The results are shown in Table 1. The histogram for the case of σ_r=80, 130 and 210 MPa, and the logarithmic mean value of the N_p for each stress range are shown in Fig. 6. In the region of high stress range, the coefficients of variance are low and the N_p shows log-normal distribution. In the stress range from 45 to 70 MPa, the number of non-failure data increases and the distribution of N_p is distorted towards the left. Especially for the case of σ_r=45 MPa, 99 percent of the data becomes runout, and this stress range level can be regarded as the fatigue limit.

The results of the simulation were compared with the experimental results of 119 as-welded specimens with plate thickness between 9 and 12 mm (87 specimens failed among them). The data was obtained from the similar specimens as the analytical model. Fig. 7 shows the test data, the S-N diagram computed by the least square method, and the mean and the mean-2s S-N diagrams of the computed N_p. The test data shows higher mean S-N diagram and wider scatter band than the simulation results. It may be due to the ignorance of fatigue crack initiation life, N_c, and/or due to the fact that the test specimens had better weld toe profiles and the initial conditions than what were assumed in the analysis. However, the simulation results were within the scatter band of the test data. Moreover, the lower bound of the computed N_p

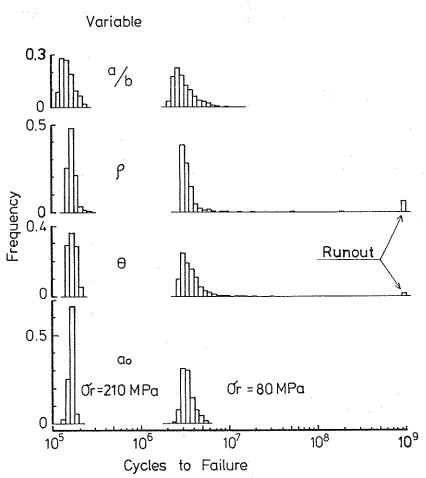

Fig. 5 Effect of various parameters on the fatigue crack propagation life.

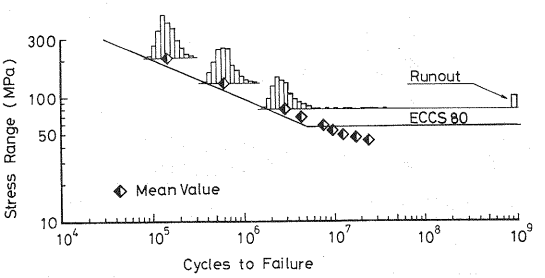

Fig. 6 Histograms and mean values obtained from simulation.

Table 1 Computed distribution of log N_p of non-load-carrying fillet welded specimens with 10 mm plate thickness. The runout data is not included.

σ r	210	130	80	70	59	55	50	48	45
Maximum Value	5.44	6.14	Runout	Runout	Runout	Runout	Runout	Runout	Runout
Minimum Value	4.98	5.57	6.22	6.39	6.62	6.71	6.90	6.93	7.04
Range	0.46	0.57	——	——	——	——	——	——	——
Mean Value	5.17	5.79	6.45	6.64	6.88	6.98	7.09	7.24	7.37
Standard Deviation	0.09	0.10	0.14	0.16	0.17	0.21	0.17	0.34	0.31
Variance Coeff.	0.0173	0.0172	0.0224	0.0247	0.0250	0.0306	0.0241	0.0464	0.0423
Skewness Coeff.	0.40	0.48	2.49	2.44	3.29	2.78	3.64	2.69	1.09
Ratio of Runout	0.00	0.00	0.07	0.27	0.62	0.78	0.92	0.96	0.99

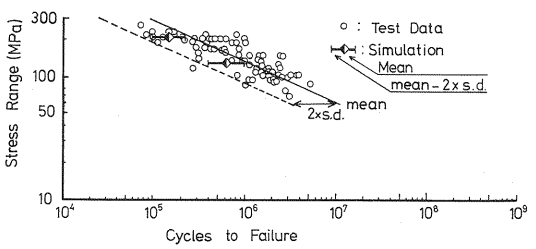

Fig. 7 Comparison between simulation results and test results of specimens with similar dimension.

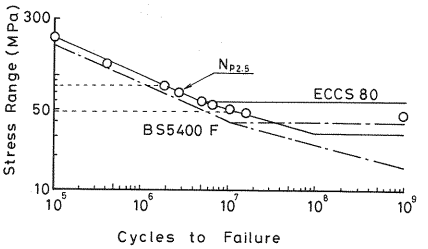

Fig. 8 Comparison between the simulated lower bound ($N_{p2.5}$) and the allowable S-N diagrams specified in ECCS and BS 5400.

represent well the tendency of the mean-2s S-N diagrams, which is important in the formulation of allowable S-N diagrams. For the case of $\sigma_r<80$ MPa, log-normal distribution is not appropriate since the runout data exist and the distribution is distorted towards the left. Thus, the lower bound was assumed to be the 25th value from the lowest value of 1 000 simulations, $N_{p2.5}$ (2.5 percent failure).

The computed $N_{p2.5}$ are shown in Fig. 8. Comparing $N_{p2.5}$ with the ECCS design S-N diagram, they are comparable at $\sigma_r=50-80$ MPa. The $N_{p2.5}$ value is slightly higher, but the fatigue limit is lower, when $\sigma_r<50$ MPa. Actually, the constant amplitude fatigue limit at five million cycles is 59 MPa in ECCS, while the simulation shows 48 MPa at 20 million cycles. The computed constant amplitude fatigue limit is about 20 percent less than the value specified by the ECCS Fatigue Recommendation[3].

4. EVALUATION ON LONGITUDINAL FILLET WELDS IN WELDED GIRDER

(1) Analytical model of blowholes in welded girder

As shown in Fig. 9(a), fatigue cracks in welded beams initiate at the blowholes in the longitudinal fillet weld root between the flange and web or at the surface of the fillet welds. Normally the fatigue life is shorter when cracks are emanating from the blowholes than when cracks are emanating from the surface. Circular cracks (penny shape) are assumed in order to compute the fatigue crack propagation life[7),13)].

Hirt et al. projected the blowhole to a plane perpendicular to the applied stress and obtained the equivalent circular crack which gives equivalent ΔK for the elliptical crack. On the other hand, Miki et al. pointed out that when the blowhole was converted into an ellipse, the fatigue life estimation would be too conservative[13)]. They suggested that the blowholes should be regarded as an ellipsoid and the equivalent radius r_e was given as follows.

$$r_e=0.80\,W^{0.057}H^{0.616}/2 \quad \cdots\cdots (8)$$

where W and H are the width and height of the blowhole perpendicular to the applied stress. Fukazawa carried out fatigue tests of large scale welded box girders and sketched the dimension, shapes and positions of fatigue cracks emanating from 53 blowholes[14)]. With these results, the equivalent radius was computed using the two methods, and the results are shown in Fig. 10. The value, r_e, by Hirt's method is about twice of that by Miki's method.

In this study, the probability distribution of the equivalent initial crack length was calculated by using Miki's approximate formula on the dimensions obtained by Fukazawa. The histogram and probability distribution are shown in Fig. 11. The probability distribution was given by the normal distribution. The mean value of this distribution was 0.88 mm and the upper and the lower cutoff were at 1.36 mm and 0.30 mm, respectively.

(2) Distribution of blowholes in the longitudinal welds

In a welded girder several cracks normally initiate and propagate in the longitudinal fillet welds. A crack of maximum size among them causes final failure and determines the fatigue life. Fukazawa observed approximately eight cracks along 1 m length of weld. The fatigue crack propagation analysis was carried

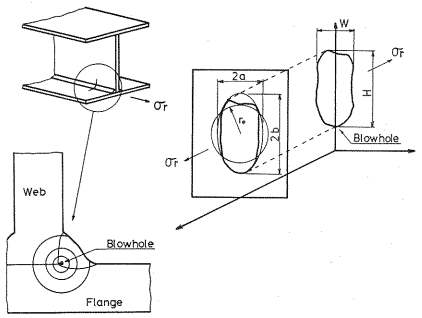

Fig. 9 Model of fatigue crack growth from blowholes in longitudinal fillet weld of welded beams.

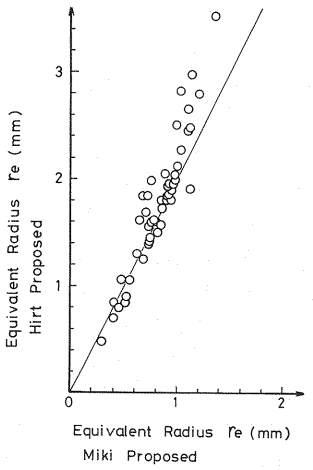

Fig. 10 Comparison of the equivalent crack sizes computed by two methods.

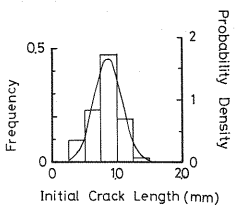

Fig. 11 Distribution of initial crack sizes used in the analysis.

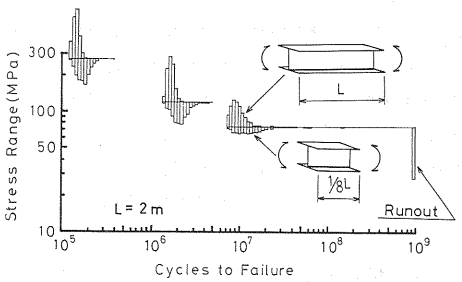

Fig. 12 Computed N_p of welded beams of 2 m long (the upper histogram) and 0.25 m long (the lower histogram).

out on a member of 2 m long of uniform moment region by assuming that only the largest one out of sixteen blowholes in 2 m long weld causes fatigue failure. The results are shown by the upper histograms in Fig. 12. In a similar way as the case of non-load-carrying fillet welded joints, the coefficient of variance varies little in high stress range region and the distribution of the N_p is distorted toward the right in low stress ranges. When σ_r=60 MPa, 99 percent of the data becomes runout and thus this value can be regarded as the computed fatigue limit. The ECCS Fatigue Design Recommendation specifies it as 40 MPa[3].

(3) Influence of weld length

If the welding is carried out under the same conditions for longitudinal fillet welded joints, the number of blowholes per unit weld length can be regarded the same along the whole weld length. Consequently, the number of blowholes in small model can be expected to be small. The simulation was carried out on a small model with the fillet weld length being one eighth of the previous model, that is 0.25 m. The results are shown by the lower histograms in Fig. 12. The lower bound of the N_p of the 0.25 m long model is about the same as that of the 2 m long model, while the mean value of the N_p of the small model is larger than that of the 2 m long model. The small model shows more runout data than the 2 m long model, for example at σ_r= 74 MPa. The results indicate the necessity of fatigue tests of sufficiently long test specimens, if one ought to examine the mean fatigue life, especially in the region of lower stress range.

5. SUMMARY

Fracture mechanics and the Monte Carlo simulation technique were used to investigate the scatter of fatigue crack propagation life. For two kinds of welded joints, the probability distribution of the influential parameters that affect the scatter of fatigue life, such as initial crack length, crack shape, flank angle and weld toe radius were estimated based on the experimental results. The Monte Carlo simulation technique was used to give initial condition to the analysis. Then the fatigue crack propagation life, N_p, was calculated by a fracture mechanics method considering the effect of the threshold value of ΔK. The results are summarized as follows.

(1) The parameter that affects the scatter of fatigue life of non-load-carrying fillet welded joints depends on the applied stress range. The fatigue life is largely affected by the crack shape in high stress range, where the ΔK_{th} has little influence. It is mainly affected by the toe radius in lower stress range where the influence of the ΔK_{th} starts appearing. The initial crack length is also the dominant factor in the low stress range where the ΔK_{th} becomes influential.

(2) The computed N_p was within the scatter band of test data. The mean and the standard deviation of test data are higher than the simulation results. The analysis shows the comparable lower bound value with 95 percent confidence interval of the test data.

(3) In the lower stress range level where the fatigue life increases or runout data increases due to the influence of ΔK_{th}, the lower bound value of the fatigue life with 95 percent confidence interval can be evaluated by taking the 25th value (0.025×number of simulation). The result is generally in good agreement with the design S-N diagram specified by ECCS. But the computed constant amplitude fatigue limit is smaller than that of ECCS.

(4) For the longitudinal fillet welded joints in welded girders, the computation was carried out by changing the length of the welds, and hence the number of blowholes. The analysis on the 2 m long model and the 0.25 m long model showed that the scatter in the computed N_p was different from each other, but showed the same lower bound values.

ACKNOWLEDGEMENT

This study was partly supported by the Grant-in Aid for Scientific Research from the Japanese Ministry of Education, Science and Culture. Much help was received from Messrs. T. Shinoda, S. Tsumagari and Ma Zhiliang of the Department of Civil Engineering, Nagoya University, for preparing manuscript. Their assistance is greatly acknowledged.

REFERENCES

1) Nomura, T. : Application of Fatigue Test Database to LRFD, Master Thesis of the Department of Civil Engineering, Nagoya University, 1986 (in Japanese).
2) Yamada, K., Makino, T. and Kikuchi, Y. : Fracture Mechanics Analysis of Fatigue Crack Emanating from Toe of Fillet Weld, Proc. of JSCE, No. 292, pp. 1~12, 1979 (in Japanese).
3) ECCS : Recommendations for the Fatigue Design of Steel Structures, 1985.
4) British Standard Institution : Steel, Concrete and Composite Bridges, Part 10, Code of Practice for Fatigue, BS 5400, 1980.
5) National Research Institute for Metals : Fatigue Crack Propagation Properties in Arc-Welded Butt-Joints of High Strength Steels for Welded Structures, NRIM Fatigue Data Sheet Technical Document No. 3, 1984 (in Japanese).
6) Albrecht, P. and Yamada, K. : Rapid Calculation of Stress Intensity Factors, Proc. of ASCE, Vol. 103, No. ST 2, pp. 377~389, 1977.
7) Yamada, K. and Hirt, M. A. : Parametric Analysis of Fatigue Life Using Fracture Mechanics, Proc. of JSCE, pp. 55~64, 1982 (in Japanese).
8) Tagaki, N., Kondo, A., Yamada, K. and Kikuchi, Y. : Influence of Fillet Weld Toe Shape on Fatigue Life of Welded Joints, Proc. of JSCE, No. 324, pp. 151~159, 1982 (in Japanese).
9) Engesvik, K. M. and Moan, T. : Probabilistic Analysis of the Uncertainty in the Fatigue Capacity of Welded Joints, Engineering Fracture Mechanics, Vol. 18, No. 4, pp. 743~762, 1983.

10) Engesvik, K. M. : Analysis of Uncertainties in the Fatigue Capacity of Welded Joints, Report VR-82-17, The Norwegian Institute of Technology, 1981.
11) Japan Road Association : Standard Specification for Highway Bridges, 1980 (in Japanese).
12) Hirt, M. A. : Fatigue Behavior of Rolled and Welded Beams, Ph. D. dissertation, Lehigh University, 1971.
13) Miki, C., Mori, T., Sakamoto, K. and Sasaki, R. : Analysis of Fatigue Crack Propagation from Root of Longitudinal Welds, Journal of Structural Engineering, Vol. 32 A, pp. 11～23, 1986 (in Japanese).
14) Fukazawa, M., Natori, A., Terada, H. and Akashi, S. : Fatigue Strength of Corner Joints after Reduction of Residual Stresses, Japan Welding Society FS-657-84, 1984 (in Japanese).
15) Yamada, K. and Hirt, M. A. : Fatigue Life Estimation using Fracture Mechanics, IABSE Report, Vol. 37, pp. 361～368, 1982.

(Received April 4 1988)